

System-Level Vulnerability Analysis for Commutation Failure Mitigation in Multi-infeed HVDC Systems

Minhan Yoon* and Gilsoo Jang[†]

Abstract – This paper deals with commutation failure of the line-commutated converter high voltage direct current (LCC HVDC) system caused by a three phase fault in the ac power system. An analytic calculation method is proposed to estimate the maximum permissible voltage drop at the LCC HVDC station on various operating point and to assess the area of vulnerability for commutation failure (AOV-CF) in the power system based on the residual phase voltage equation. The concept is extended to multi-infeed HVDC power system as the area of severity for simultaneous commutation failure (AOS-CF). In addition, this paper presents the algorithm for the implementation of a shunt compensator applying to the proposed method. An analysis and simulation have been performed with the IEEE 57 bus sample power system and the Jeju island power system in Korea.

Keywords: HVDC, Multi-infeed, LCC, Commutation failure, Power system

1. Introduction

The modern power system has been widely implementing large-scale and long-distance transmission, asynchronous interconnection, inter-area interconnection, and renewable energy integration by using HVDC systems [1-3]. Consequently, several HVDC converter stations of the system would be closely located in a power system. In this multi-infeed HVDC systems, interactions between systems are required to be analyzed for the stable power system operation in terms of voltage stability, and reliability criteria [4-6]. These criteria must be handled especially with LCC HVDC. In addition, the commutation failure phenomenon caused by voltage fluctuation in the ac system is another weakness of LCC HVDC [7]. IEEE and Cigre have reported the documents about implementation and operation of HVDC system [8-11].

The commutation failure mainly occurs due to a sudden ac voltage drop at the inverter station, and it is commonly seen with a weak ac power system. During a commutation failure, the dc voltage of the HVDC system drops to zero. This phenomenon quickly leads to loss of the power that flows through the HVDC system. In case of simultaneous commutation failure in a multi-infeed system, a large portion of the power generation into the system may be lost.

To analyze commutation failure, the EMT-based simulation is typically utilized. E. Rahimi proposed the commutation failure immunity index (CFII) by the multiple-run electro-magnetic transient (EMT) simulation method [16]. He verified the relationship between the system strength and the commutation failure in multi-

infeed HVDC systems [17]. X. Chen generalized the solution to an indexed commutation failure effective short-circuit ratio (CFESCR) [18]. However, the method is not applicable for remote faults at specified points in power system.

The EMT-based approach has an advantage in the accuracy point of view and the dynamics of the device response with transient phenomenon can be reflected. However, the error between the analytic method and the EMT-based simulation is within a few percentages [19]. However, the computation time of EMT-based simulation is hundreds of times compared to analytic method. Consequently, the simulation with an empirical EMT-based simulation is not widely used for large-scale power system. Therefore, to analyze the vulnerable area for commutation failure in the power system, it is difficult to apply the critical distance method and fault position methods based on empirical simulation with the large-scale meshed networks

The assessment of system voltage sag performance on the area of vulnerability (AOV) based on residual phase voltage equations was introduced by C. Park [20]. This concept extends to the area of severity (AOS) to determine the vulnerable area for multi-sensitive loads [21-23]. The method verified the relationship between the voltage fluctuation at specified bus and the fault location and has been utilized to analyze power system equipment in voltage sag study [24, 25].

To ensure a stable multi-infeed system operation from simultaneous commutation failure, this paper proposes analyzing the critical voltage drop or severity of the fault leading to commutation failure using analytic method and estimating the area vulnerable to simultaneous commutation failure in multi-infeed system. In this paper, a method to estimate vulnerable areas for simultaneous

[†] Corresponding Author: School of Electrical Engineering, Korea University, Seoul, Korea. (gjang@korea.ac.kr)

* Department of Electrical Engineering, Tongmyong University, Busan, Korea. (minhan.yoon@gmail.com)

Received: January 20, 2016; Accepted: November 4, 2017

commutation failure in multi-infeed systems for the three-phase fault, most severe disturbance for voltage depression, is proposed.

To mitigate commutation failure, several studies have been performed in the control point of view. [12-14]. Otherwise, an alternative approach is possible from the ac system compensation. The effect of the shunt compensator on the prevention of commutation failure was recently presented [15]. In this paper, an equivalent modeling method presented to apply the shunt compensator for the assessment of the area of severity (AOS). The proposed methods were case studied on the IEEE 57 bus test system and the Jeju island power system in Korea, where the real multi-infeed HVDC systems exist.

2. Analysis of the Commutation Failure

In this paper, the analytic calculation method is utilized to determine the critical voltage drop limit for commutation failure analysis. It is possible to identify the critical conditions for commutation failure at inverter stations regarding the amount of critical voltage drop required to induce the commutation failure analytic calculation [19].

The basic dc current equation (I_d) can be derived with the AC bus voltage connected to valves (E), commutating reactance (X_c), ignition firing angle (α) and extinction angle (γ) as follows.

$$I_d = \frac{E}{\sqrt{2}X_c}(\cos \alpha + \cos \gamma) \tag{1}$$

When the AC bus voltage reduced (E'), overlapped angle increases (μ') and extinction angle decreases (γ') as shown in Fig. 1. As this time, the dc current (I') changes (2).

$$I'_d = \frac{E'}{\sqrt{2}X_c}(\cos \alpha + \cos \gamma_0) \tag{2}$$

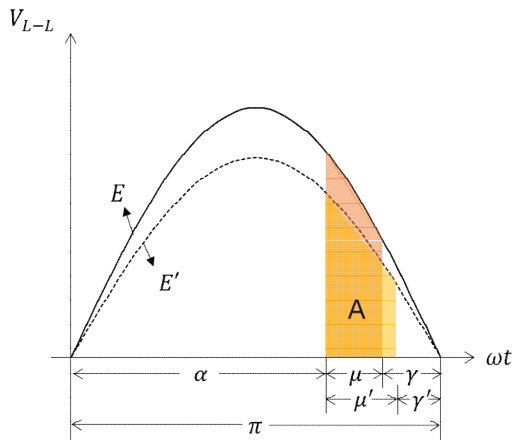


Fig. 1. The effect of voltage reduction to commutation margin

Through the (1) and (2), the relationship between the commutating voltage before and after the disturbance can be derived.

$$\frac{E'}{E} = \frac{I'_d \cos \alpha + \cos \gamma}{I_d \cos \alpha + \cos \gamma_0} \tag{3}$$

From (1), the inverter firing angle is expressed as

$$\cos \alpha = \frac{\sqrt{2}I_d X_c}{E} - \cos \gamma \tag{4}$$

If we substitute firing angle equation into (3), for the symmetrical three-phase fault, which is most severe condition for commutation, the critical voltage drop that draw the extinction angle to critical extinction limit ($\gamma = \gamma_0$) can be calculated as shown in (5). The critical voltage drop leading to commutation failure is being affected by dc current change due to a fault (I_d / I'_d), operation current point versus rated DC current (I_d / I_{dFL}) and extinction angle (γ). The full-load voltage (E_{FL}) is almost equal to the operation voltage in typical power system operation voltage, then, (E_{FL} / E) is assumed to be unity.

$$\Delta V = 1 - \frac{I_d \left(\frac{I_d}{I_{dFL}} \right) \cdot X_{cpu}}{I'_d \left(\frac{I_d}{I_{dFL}} \right) \cdot X_{cpu} + \cos \gamma_0 - \cos \gamma} \tag{5}$$

In a fault situation, the dc current change ratio (I_d / I'_d) is assumed to be stabilized by the constant current control of HVDC and a sufficiently large capacity of smoothing reactor. Based on the assumption, the critical voltage drop formula can be simplified as (6),

$$\Delta V = 1 - \frac{I_{dpu} \cdot X_{cpu}}{I_{dpu} \cdot X_{cpu} + \cos \gamma_0 - \cos \gamma} \tag{6}$$

The determination of a current operation point is performed by a system operator considering load level, generation, and transmission facility status, etc. Normally, the HVDC operation extinction angle is between 20~30 degrees for securing the commutation margin to avoid commutation failure. The internal controller of the HVDC system sets the extinction angle considering other control loops with various transfer functions [7].

Fig. 2 shows the result of critical voltage drop according to the change of dc current and extinction angle operation point. Several representative values of critical voltage drop, which is varied by HVDC current and extinction angle operation points, are shown in Table 1. The commutating reactance (X_{cpu}) is assumed to be 0.2, and the critical extinction angle (γ_0) is set to the ideal value, zero. The

Table 1. Critical voltage drop depending on HVDC operation point

Operation current point (I_{dpu})	Operation extinction angle (γ)		
	20°	25°	30°
0.1	0.80	0.86	0.90
0.4	0.50	0.61	0.69
0.7	0.36	0.47	0.56
1.0	0.29	0.38	0.47

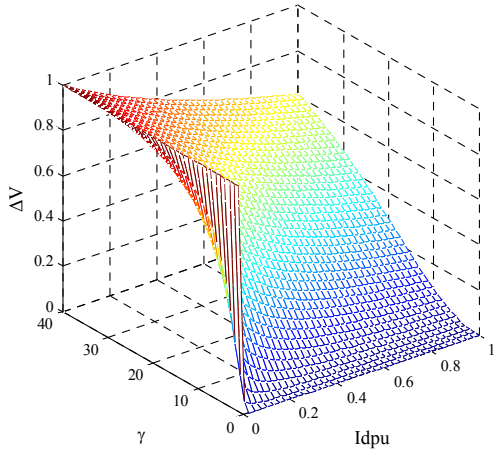


Fig. 2. Critical voltage drop analysis versus the operation current point and extinction angle

critical voltage drop increases with the decrease of the current operation point (I_d / I_{dFL}). On the other hand, the critical voltage drop increases with the increase of the extinction angle (γ). Therefore, the full-load operation with small commutation margin is a vulnerable condition that can trigger commutation failure.

3. Analysis of the Vulnerable Area

3.1 The method for finding critical points

The magnitude of voltage sag can be derived from the impedance matrix and residual phase voltage equations [20, 23]. To calculate the voltage drop at converter station m , the equivalent driving-point impedance (Z_{kk}) and transfer impedance between the converter station m and the fault position K (Z_{mk}) are required. The procedure to derive the fault position in the length of a line p is based on the quadratic formula and the secant method. These impedance can be derived as follows

$$Z_{mK} = Z_{mF} + (Z_{mT} - Z_{mF})p \quad (7)$$

$$Z_{KK} = (Z_{FF} + Z_{TT} - 2Z_{TF} - Z_C)p^2 + (Z_C - 2(Z_{FF} - Z_{FT}))p + Z_{FF} \quad (8)$$

V_F^{pref} is the pre-fault voltage at the sending end, and V_T^{pref} is the receiving end bus voltage of the line. When

considering pre-fault voltages of the buses on both ends of the line, the pre-fault voltage at fault position K can be expressed as follows:

$$V_k^{pref} = V_F^{pref} + (V_T^{pref} - V_F^{pref})p \quad (9)$$

Through the ratio of the impedance between the bus m and position K (Z_{mk}) and the thevenin equivalent impedance at position K (Z_{KK}), the voltage drop at bus m is possible to be calculated. Finally, the residual phase voltage at the specified bus m when a three-phase symmetrical fault occurs at fault position K can be derived as follows:

$$|V_m^{fault}| = \left| V_m^{pref} - \frac{Z_{mK}}{Z_{KK}} \cdot V_k^{pref} \right| = \left| V_m^{pref} - \Delta V_m \right| \quad (10)$$

By substituting the voltage drop at the bus m with the critical voltage drop at the converter bus, it is possible to derive the critical fault position p where the three-phase fault occurs, leading to commutation failure.

3.2 The concepts of the area of vulnerability and the area of severity

As mentioned in Section 3.1, the critical points p where the occurrence of fault cause over the specific voltage sags at the bus m can be calculated based on the impedance matrix and residual phase voltage equations. The critical points are the boundary of the area of vulnerability (AOV). At anywhere in the region, the three phase line-to-ground fault drop the voltage at bus m less than V_m^{fault} . In other words, the magnitude of voltage sag at bus m is over ΔV_m .

Fig. 3 shows the three fault position A, B, C and the AOV for bus 1 and bus 2 and the area of severity (AOS). The three-phase fault at the point A lead to the voltage sag over ΔV_{m1} at bus 1, however, the voltage sag at bus 2 is

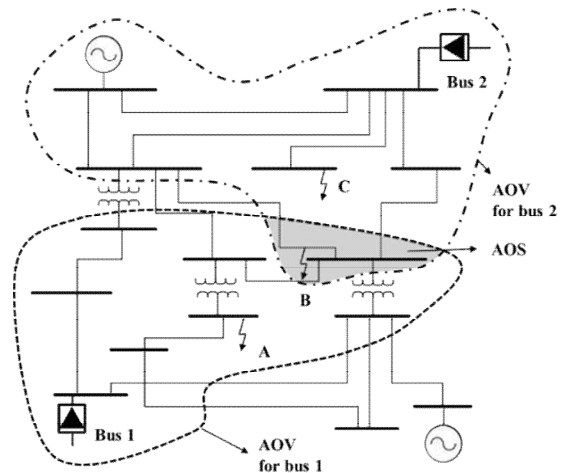


Fig. 3. The schematic diagram of AOV and AOS for commutation failure

below ΔV_{m2} .

On the other hand, the fault at the point C lead to the voltage sag over ΔV_{m2} at bus 2, however, not over ΔV_{m1} at bus 1. The occurrence of a three-phase fault at B point reduce the voltages both of bus 1 and bus 2 over ΔV_{m1} and ΔV_{m2} . This overlapped shaded area is defined as the AOS. Reference [21] contains more detailed explanation of the AOS.

3.3 Analysis of the AOV-CF

To determine the area of vulnerability for commutation failure (AOV-CF), the critical voltage drop of the LCC HVDC station bus has to be analyzed firstly. These results affect the change of the critical fault position and the AOV. Through the approach described in Section 2, the AOV-CF assessment is available for various operation points. The

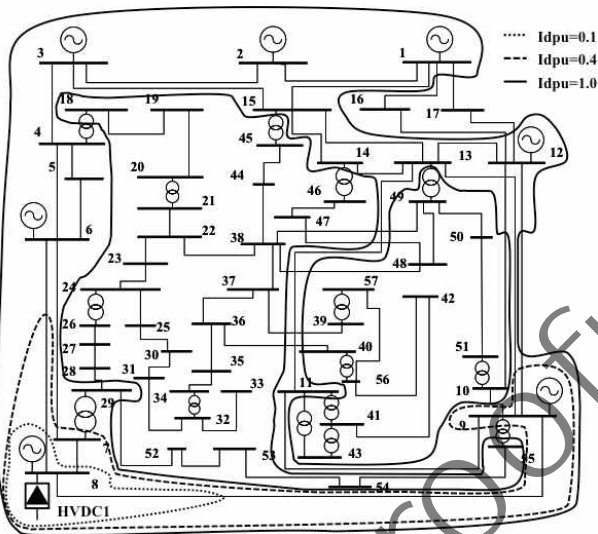


Fig. 4. AOV-CF depending on the varied operation current

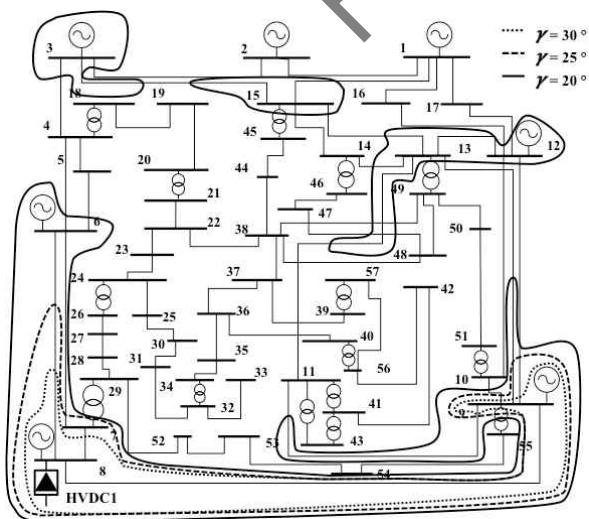


Fig. 5. AOV-CF depending on the varied operation extinction angles

large critical voltage drop means strong immunity against commutation failure. It leads to a small vulnerable area.

For HVDC 1, which is connected to bus 8, Fig. 4 shows the changes in AOV-CF due to changes in current operation point (I_{dpu}). As shown in Fig. 4, The AOV-CF is smaller with the lower current operation point. In Fig. 5, the change of AOV-CF versus the extinction angle margin is shown. The AOV-CF is smaller, with a sufficient extinction angle margin to critical extinction angle.

3.4 Analysis of the AOS-CF

The each area of vulnerability for commutation failure (AOV-CF) of HVDC systems can be calculated by applying (10) to each of converter station buses in the multi-infeed system. Consequently, the area of severity for simultaneous commutation failure (AOS-CF) is determined by the overlapped area of each AOV-CF. In Fig. 6, HVDC 1 is connected to bus 8, and HVDC 2 is connected to bus 17. Both HVDCs are assumed to be operated at rated current point of 1.0 and inverter extinction angle of 25 degrees. There is an overlapped area of AOV-CF1 and AOV-CF2.

When the three-phase fault is applied in this overlapped area, the voltage drop at HVDC 1 converter station bus (bus 8) and HVDC 2 converter station bus (bus 17) exceeds each of the critical voltage drop. At this time, simultaneous commutation failure occurs, consequently, the system loses the generations from two HVDCs during commutation failure.

3.5 Shunt compensator application

The shunt compensators such as the synchronous condenser, static var compensator (SVC), and static synchronous compensator (STATCOM) are able to regulate reactive power to provide voltage support when a contingency occurs. In case of implementing these compensators, the

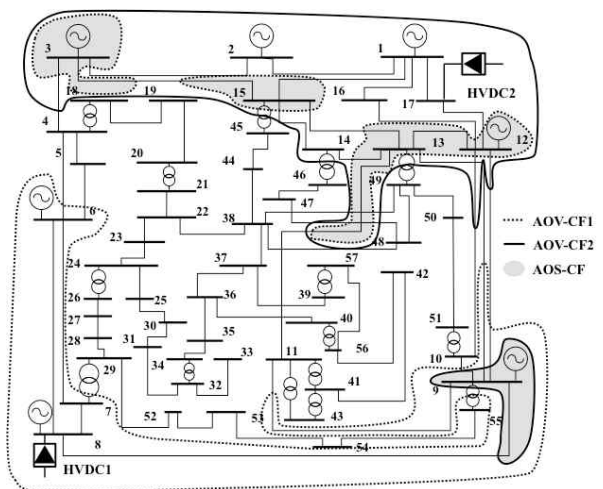


Fig. 6. AOS-CF considering two HVDC converter station

size of the AOV-CF or AOS-CF can be apparently changed.

In this study, the compensator is applied for analysis since it has rapid response capability. To simulate the shunt compensator in AOV-CF analysis, the equivalent modeling as reactive power source has to be performed. The compensators can be modeled using equivalent impedance (X_{st}) and voltage sources. [26, 27].

Sequentially, the AOV-CF decreases by implementing the shunt compensators and its impedances.

4. Case Study

4.1 Introduction of Jeju island power system

Jeju Island system in Korea is an isolated power system which is separate from the mainland. The system has a low short circuit capacity, and two LCC HVDCs are installed to supply the power demand. The peak-load demand was approximately 820MW in 2014, and a large portion of the power is supported by two HVDCs [29].

In this situation, simultaneous commutation failures can cause a large amount of generation outage. Analysis of the fault leading to simultaneous commutation failure and the solution for this problem is essential. The STATCOM has

been installed closed to be each converter station, Jeju C/S and W-Jeju S/S for the voltage compensation. The capacity of STATCOMs are set to 50MVA as a generic size.

The specifications of the HVDCs are presented in Table 2. The total rated capacities of two HVDCs are 700MW. However, under normal conditions, the total transfer capacity of two HVDCs is 400MW (#1 HVDC 150MW and #2 HVDC 250MW). It is the operation strategy of the Korean power system operator to secure N-1 reliability [28].

4.2 AOS-CF analysis of #1 & #2 HVDC system

Critical voltage drop is calculated as 0.55 pu for #1 HVDC operation with 150MW transfer capacity and minimum extinction angle ($\gamma_{\#1HVDC} = 23.5^\circ$). For #2 HVDC with 250MW transfer capacity with minimum extinction angle operation ($\gamma_{\#2HVDC} = 21^\circ$), critical voltage drop is 0.29 pu. In Fig. 8, the AOV-CF of each converter station with minimum extinction angle operation point is described by the proposed method. The AOV-CF of the #1 HVDC is presented in a wide area in the Jeju system.

With the #2 HVDC, the AOV-CF covered the whole power system. As mentioned above, the system is too weak to maintain stable operation from commutation failure.

This value can be alleviated by loosening the operation extinction angle ($\gamma_{\#1HVDC} = 30^\circ$). As a result, the critical voltage drop of #1 HVDC station bus increases to 0.67 pu. For #2 HVDC, the critical voltage drop increases to 0.48 pu ($\gamma_{\#2HVDC} = 30^\circ$). As shown in Fig. 9. The southern and eastern area of Jeju island system is excluded from AOS-CF. However, a large portion of the northern area is still vulnerable to faults, leading to simultaneous commutation failure.

Table 2. HVDC specification in Jeju island

	HVDC Bipole 1	HVDC Bipole 2
Power Rating	150 [MW] × 2 (Bipoles)	200 [MW] × 2 (Bipoles)
Voltage	184 [kV]	250 [kV]
Current	815.2 [A]	800 [A]
Impedance of Transformer	7.999 [ohm]	14.73 [ohm]
Gamma Firing Angle minimum (Inverter)	23.5 [deg]	21 [deg]
Critical extinction angle	8 [deg]	

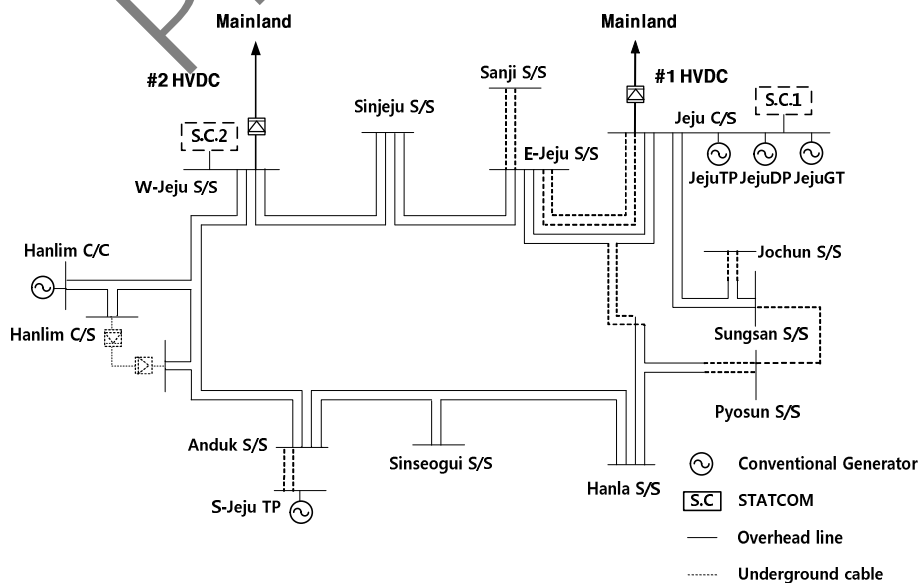


Fig. 7. Jeju island power system schematics

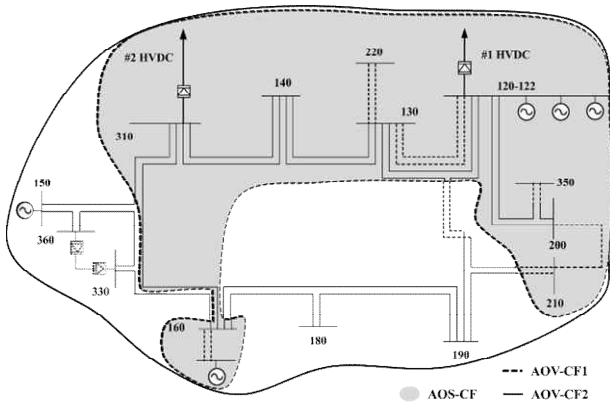


Fig. 8. AOS-CF with minimum γ operation

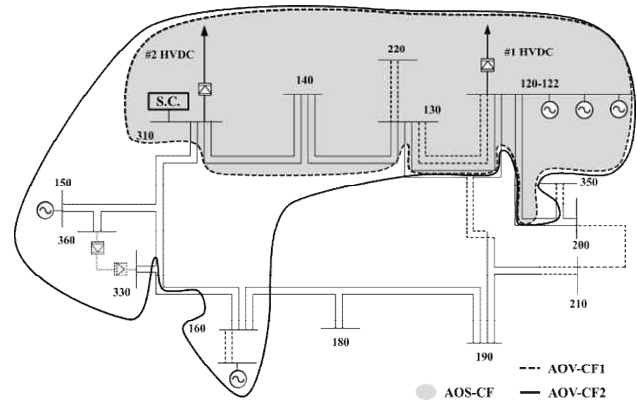


Fig. 11. AOS-CF with #2 shunt compensator installation

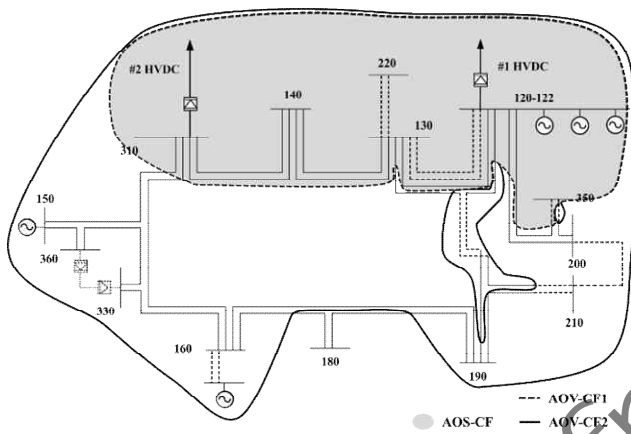


Fig. 9. AOS-CF when $\gamma = 30^\circ$

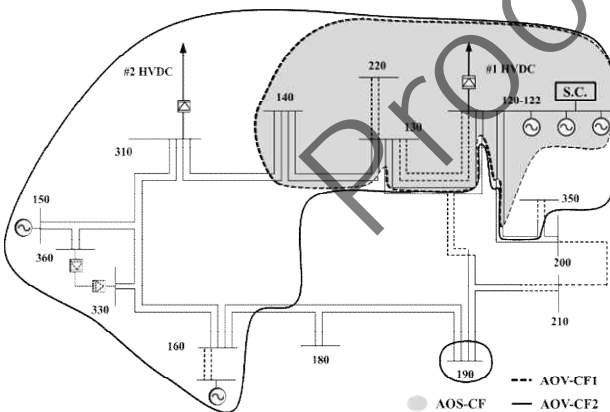


Fig. 10. AOS-CF with #1 shunt compensator installation

4.3. AOS-CF with shunt compensator installation

After 100MVA shunt compensator installation at the HVDC converter station at Jeju C/S (Case 1) and W-Jeju S/S (Case2) buses, the AOV-CF of #2 HVDC was reduced dramatically as shown in Fig. 10 and 11. The reduction of AOV-CF by shunt compensator installation is most significant when it is installed at each of HVDC converter station buses. From the AOS-CF point of view, shunt

compensator installation at #1 HVDC converter bus is more efficient for preventing simultaneous commutation failure since AOS-CF is smaller.

6. Conclusion

This paper presented a method to analyze the area of vulnerability for commutation failure by the three-phase fault based on an analytical approach. Sequentially, the area of severity for simultaneous commutation failure is analyzed for multi-infeed HVDC systems. The method is an analytical approach to identify the fault position leading to simultaneous commutation failure. It has an advantage in rapid analysis time without a detailed device modeling or a complicated large-scale meshed system modeling used in empirical EMT-based simulation. Furthermore, the analytic model can be easily applied and expanded to other fields of power system analysis. The proposed method looks forward to be usefully utilized in real-time monitoring system, control strategy establishment for preventing undesired damage, and long-term power system planning.

Acknowledgements

This research was supported by Korea Electric Power Corporation. (R17XA05-4) and Tongmyong University Research Grants (2017A004)

References

- [1] S. K. Chaudhary, R. Teodorescu, and P. Rodriguez, "Wind farm grid integration using VSC based HVDC transmission-an overview," in *Energy 2030 Conference, ENERGY 2008. IEEE*, 2008, pp. 1-7.
- [2] B. Kahinpour, "Modelling, control and investigation of an HVDC transmission for an offshore wind farm," *Master of Science Thesis*, Chalmers University of

- Technology, 2009.
- [3] S. M. Muyeen, R. Takahashi, and J. Tamura, "Operation and Control of HVDC-Connected Offshore Wind Farm," *IEEE Transactions on Sustainable Energy*, vol. 1, pp. 30-37, Apr 2010.
- [4] R. Nayak, R. Sasmal, Y. Sehgal, and S. Mukoo, "AC/DC interactions in multi-infeed HVDC scheme: a case study," *Power India Conference, 2006 IEEE*
- [5] S. Lee, M. Yoon, A Study on the Operation Strategies of Multi-Infeed HVDC System in Jeju Island Power System, vol. 66, no. 12, pp. 1675~1681, 2017
- [6] D. L. H. Aik and G. Andersson, "Analysis of Voltage and Power Interactions in Multi-Infeed HVDC Systems," *IEEE Transactions on Power Delivery*, vol. 28, pp. 816-824, Apr 2013.
- [7] C.-K. Kim, V. K. Sood, G.-S. Jang, S.-J. Lim, and S.-J. Lee, HVDC transmission: power conversion applications in power systems: John Wiley & Sons, 2009.
- [8] G. Andersson, "Commutation Failure Causes and Consequences," Cigre TB 103 SC 14 WG 14.05, 1996.
- [9] P. Krishayya, Adapa, R, Holm, M, "IEEE guide for planning DC links terminating at AC locations having low short-circuit capacities, part I: AC/DC system interaction phenomena," *IEEE Std 1204-1997*, 1997.
- [10] S. Henry, "Influence of Embedded HVDC Transmission on System Security and AC Network Performance," Cigre JWG C4/B4/C1.604, 2013.
- [11] "IEEE Guide for the Evaluation of the Reliability of HvdC Converter Stations," IEEE Std 1240-2000, p. i, 2001.
- [12] A. Hansen and K. Havemann, "Decreasing the commutation failure frequency in HVDC transmission systems," *IEEE Transactions on Power Delivery*, vol. 15, pp. 1022-1026, Jul 2000.
- [13] L. Zhang and L. Dofnas, "A novel method to mitigate commutation failures in HVDC systems," in *Proceedings of PowerCon 2002*, 2002, pp. 51-56.
- [14] J. Bauman and M. Kazerani, "Commutation failure reduction in HVDC systems using adaptive fuzzy logic controller," *IEEE Transactions on Power Systems*, vol. 22, pp. 1995-2002, Nov 2007.
- [15] M. Khatir, S. A. Zidi, M. K. Fellah, S. Hadjeri, and M. Flitti, "The Impact Study of a Statcom on Commutation Failures in an HvdC Inverter Feeding a Weak Ac System," *Journal of Electrical Engineering-Elektrotechnicky Casopis*, vol. 63, pp. 95-102, Mar-Apr 2012.
- [16] E. Rahimi, S. Filizadeh, and A. Gole, "Commutation Failure Analysis in HVDC Systems using Advanced Multiple-run Method," in *International Conference on Power Systems Transients*, 2005, pp. 19-23.
- [17] E. Rahimi, A. Gole, J. Davies, I. Fernando, and K. Kent, "Commutation failure in single-and multi-infeed HVDC systems," in *ACDC 2006*, 2006.
- [18] X. Y. Chen, A. M. Gole, and M. X. Han, "Analysis of Mixed Inverter/Rectifier Multi-Infeed HVDC Systems," *IEEE Transactions on Power Delivery*, vol. 27, pp. 1565-1573, Jul 2012.
- [19] C. Thio, J. Davies, K. Kent, and G. ANDERSSON, "Commutation failures in HVDC transmission systems. Discussion," *IEEE transactions on power delivery*, vol. 11, pp. 946-957, 1996.
- [20] C. H. Park and G. Jang, "Stochastic estimation of voltage sags in a large meshed network," *IEEE Transactions on Power Delivery*, vol. 22, pp. 1655-1664, Jul 2007.
- [21] C.-H. Park, J.-H. Hong, and G. Jang, "Assessment of system voltage sag performance based on the concept of area of severity," *IET generation, transmission & distribution*, vol. 4, pp. 683-693, 2010.
- [22] C.-H. Park and J.-H. Hong, "Calculation of the Area of Severity for Voltage Sag Assessment," *The Transactions of the Korean Institute of Electrical Engineering*, vol. 59, pp. 1034-1040, 2010.
- [23] C. H. Park and G. Jang, "Systematic Method to Identify an Area of Vulnerability to Voltage Sags," *IEEE Transactions on Power Delivery*, vol. 32, pp. 1583-1591, Nov 2016.
- [24] K. Lee, M. Yoon, C. Park, G. Jang, Utilization of Energy Storage System based on the Assessment of Area of Severity in Islanded Microgrid, *Journal of Electrical Engineering & Technology*, vol. 12, no. 2, pp. 569-575, Mar 2017
- [25] S. Park, M. Yoon, A Study of the Mitigating Effect Comparison of Voltage Sags by WTG Types Based on the Concept of Area of Vulnerability, Vol. 66, No. 12, pp. 1682~1688, Dec 2017
- [26] Z. Yang, C. Shen, M. L. Crow, and L. Zhang, "An improved STATCOM model for power flow analysis," in *Power Engineering Society Summer Meeting, 2000. IEEE*, 2000, pp. 1121-1126.
- [27] J.V. Milanovic and Y. Zhang. "Modeling of FACTS devices for voltage sag mitigation studies in large power systems," *IEEE transactions on power delivery*, vol. 25, pp. 3044-3052, 2010
- [28] KPX, "A Long-term view of power system operation," *KPX Technical Report*, pp. 251-268, 2013.



Minhan Yoon He received the B.S. degree and the Ph.D. degree from the Department of Electrical Engineering, Korea University, Seoul, Korea, in 2009 and 2015, respectively. He was a Post-doctoral Research Associate in Seoul National University, Seoul, Korea, in 2015, and a Senior Engineer with Korea Electrotechnology Research Institute (KERI) during 2015-2017. In 2017, he joined the Department of Electrical Engineering, Tongmyong University, Busan,

Korea, as an Assistant Professor. His research interests include power system transients and AC-DC system interactions.



Gilsoo Jang He received the B.S. and M.S. degrees in electrical engineering from Korea University, Seoul, Korea, in 1991 and 1994, respectively, and the Ph.D. degree in electrical and computer engineering from Iowa State University, Ames, in 1997. He was a Visiting Scientist at Iowa State University from

1997 to 1998 and a Senior Researcher with the Korea Electric Power Research Institute, Daejeon, Korea, from 1998 to 2000. Currently, he is a Professor in the School of Electrical Engineering, Korea University. His research interests include power quality and power system control.

proofreading